

Seismicity Relocations around the Sinai Peninsula, northeast of Egypt: Contribution of regional seismic networks

Ahmad M. Faried¹, Ahmed Hosny¹, Abd El-Naser A. Helal², Mahmoud S. El-Hadidy¹, Hani M. Zahran³, O. Novotný⁴ and Karam S. Farag²

¹Seismology department, National Research Institute of Astronomy and Geophysics (NRIAG), Helwn, Cairo, Egypt

²Geophysics Department, Faculty of Science, Ain Shams University, Cairo, Egypt.

³Saudi Geological Survey, National Center for Earthquakes and Volcanoes, Jeddah 21514, Saudi Arabia

⁴Department of Geophysics, Faculty of Mathematics and Physics, Charles University, Praha 8, Prague, Czech Republic

geo_eagle@live.com

Abstract: The area around Sinai Peninsula (including Gulf of Aqaba, Gulf of Suez, and Northern Red Sea) is considered as the most active seismic region due to its complicated geologic structures. In this area, the recent seismic activity for a period from 1997 to 2014 (1445 events) recorded by the Egyptian National seismic network (ENSN), the Saudi Arabia seismic network (SASN) and some stations located in Palestine have been relocated. Three techniques were applied for improving the seismicity locations, least square method, the Wadati diagram method, and the Probability method for the determination of earthquake epicenters. Since the waveforms of the ENSN were available, re-picking for the seismic phases was implemented via least square method to minimize the time residuals of the picked seismic phases. For the all seismic data used, physical tests for the arrivals of the P and S phases was performed using the Wadati method to obtain more reliable phase picking. The final locations were obtained using the Hypoinverse program, applying the Probability method for the determination of earthquake epicenters. The average horizontal dislocation in epicenters was measured at ~13 Km, the average Vertical dislocation in Hypocenters was ~8 Km. The relocations have been improved and revealed cluster of seismic activity around the triple junction area, particularly at the opening areas of Gulf of Suez and Gulf of Aqaba. The relocated seismicity was centered on the active faults cutting the study area. When compared with previous studies conducted on the same area, our results give good locations of seismic activity relate to the tectonic setting of the study region, since more arrivals of different networks were used. The output of this study is considered a new contribution for further seismic hazard studies by providing a more precise seismic catalogue of the instrumentally recorded events in the study region from 1997 to 2014. Hence this provided catalogue may use for any other seismological applications in future.

[Ahmad M. Faried, Ahmed Hosny, Abd El-Naser A. Helal, Mahmoud S. El-Hadidy, Hani M. Zahran, O. Novotný, and Karam S. Farag. **Seismicity Relocations around the Sinai Peninsula, northeast of Egypt: Contribution of regional seismic networks.** *N Y Sci J* 2017;10(4):37-50]. ISSN 1554-0200 (print); ISSN 2375-723X (online). <http://www.sciencepub.net/newyork>. 5. doi: [10.7537/marsnys100417.05](https://doi.org/10.7537/marsnys100417.05).

Keywords: Seismicity, Earthquakes, Sinai, Relocations, Wadati, Northeast of Egypt

Introduction

The North East of Egypt including the Sinai and the triple junction area is considered the most active seismotectonic region in Egypt due to the geologic and seismotectonic complicated structures, **Hosny et al., (2015)** and **Hosny et al., (2013)**. It is a tectonic active region and controlled by active rifting in the Red Sea, left lateral strike slip motion along the Gulf of Aqaba and Levant transform, in addition to the convergence between Africa and Eurasian in the eastern Mediterranean. Its seismic activity is characterized by large and moderate activity. Most of events are concentrated along the Gulf of Aqaba, Gulf of Suez, and in the northern part of the Red Sea.

By using only seismic stations of the Egyptian National seismic network (ENSN), the seismic activity was not located properly due to the lack of

observations and the large azimuth gap, especially events occurred in the Gulf of Aqaba and northern Red Sea. Therefore, for obtaining more proper locations, we added arrivals of the same dataset recorded by some regional seismic networks in addition to the ENSN, such as the Saudi seismic network (SSN), Israel Seismic Network (ISN) and International Monitoring System (IMS). Also, arrivals from the International Seismological Center (ISC) were used.

Additionally, the Wadati diagram (**Novotny et al., 2016**) and the least square methods were applied to enhance the phase picking and reduce its time residuals, and minimizing the horizontal and the vertical errors associated the hypocenters.

The new locations were improved and show attaching of seismicity around the active faults cutting the study area. When compared with previous studies

conducted on the same area, our results give good locations of seismic activity relate to the tectonic setting of the study region. This study provided a new catalogue of locations for the seismic activity of that active seismic zone, and as a result other seismological studies could be conducted, such as seismic hazard assessment, velocity models, or any other studies related using the new seismic catalogue.

Geologic and tectonic settings

Many previous researchers studied the geology, tectonics and kinematics of Sinai borders and northern Red Sea region (e.g. **Shata, 1956; Said, 1962; Woodside, 1977; Garfunkel, 1981; Abdel-Fattah, 1999; Bosworth and McClay, 2001; Abdel Rahman et al., 2008; and Hosny and Nyblade 2016**). It is highly dissected by igneous and metamorphic mountains, which rise to a height of 2675m (Gebel Musa) and form the southern tip of the peninsula. In the south, exposed Pre-Cambrian igneous and metamorphic rocks form the so-called Arabian-Nubian Shield, figure (1). In central Sinai lie Gebel El Tih and Egma plateau with 914m above the sea level, which is affected mainly by faulting. This region has been described in detail by **Shata (1956) and Said (1962)**.

Faults in central Sinai are of the normal type. These faults are distinguished into N-S to NNE-SSW, NW-SE and E-W trends which dominating the northern portion of the area. The centre of Sinai is characterized by a shear zone of dextral E-W strike slip faults with up to 2.5 km of displacement (**Steinitz et al., 1978**) and Raqabet El-Naam dextral fault. Northward of this zone, the style of deformation gets increasingly complex and consists predominantly of 65°N to 85°E oriented anticlinal folds and monoclinial flexures expressed mainly in the Cretaceous strata. This belt of folds extends offshore into the southeast Mediterranean Sea.

The Gulf of Suez is a northwest trending intracratonic basin separated from the Red Sea by the Aqaba Transform fault. It separates the African Plate from the Sinai sub-plate in Eastern Egypt, bounded by Sinai massive in the east bank and by the Red Sea hills of the Eastern Desert from the west. The Gulf of Suez Rift consists mainly of three tectonic provinces that are separated by two accommodation zones. The northern accommodation zone trends ENE, while the southern zone trends WNW. The main direction of faulting along the entire Gulf is N330° (the Clysmic Trend parallel to the Gulf) and N10° (the Aqaba Trend). Both of these trends may be related to pre-existing structures (**Robson, 1971**). **Steckler (1985)** estimated the total extension in the central Gulf of Suez as 25-27 km corresponding to an average extension factor (β) of 1.3. The amount of extension increases to the south.

The Levant fault zone of the Gulf of Aqaba is a major left lateral strike slip fault that accommodates the relative motion between Africa and Arabia (**Salomon, et al., 1996**). It connects a region of extension in the Northern Red Sea to the Taurus collision zone to the north. This fault zone consists of en echelon faults with extensional jogs; with the largest such step over being the Dead Sea pull-apart basin. The fault zone extends over 1000 km from the Red Sea Rift to the collision zone in Eastern Turkey. Its slip rate remains poorly constrained. Geological observations suggest a nearly pure strike slip faulting and estimated slip rates range between 1 and 20 mm/yr (**Gardosh, et al., 1990 and Ginat, et al., 1998**).

Bauer et al. (2001) conclude that the geodynamic evolution of the study region is characterized by: (1) Late Triassic–Early Jurassic rifting and opening of the Neotethyan Ocean; (2) compression since the Turonian, owing to the initial collision of the Afro-Arabian and Eurasian plates. Neotethyan rifting during the Triassic led to the formation of half grabens and basins on the ‘unstable shelf’ (**Said, 1962**) in northern Sinai (**Kuss and Lepping, 1989; Moustafa and Khalil, 1990**) and Egypt (**Kuss, 1992**).

Mart and Hall (1984) suggested that there is no indication for a triple junction neither in southern Sinai Peninsula nor in the Northern Red Sea, while others (**McKenzie, et al., 1970; Le pichon and Franchateau, 1978; and Cochran 1983**) postulated a triple junction in southern Sinai.

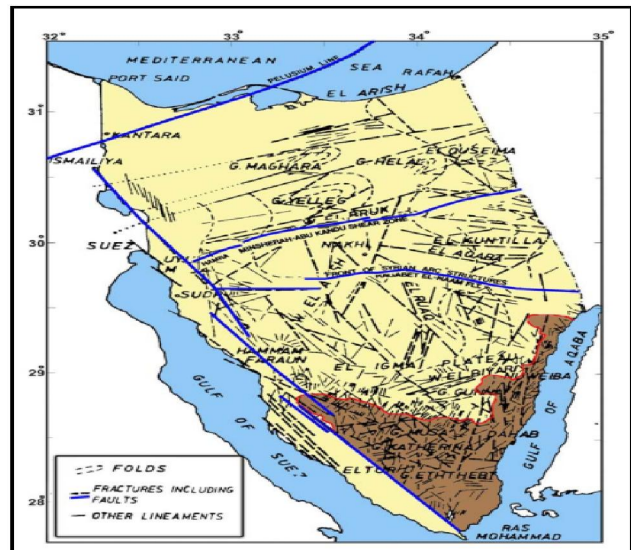


Figure (1). Geologic and tectonic map of the Sinai region, (modified after El Shazly et al., 1974; Neev, 1975 and Agath, 1981).

Seismic Data and Seismic Networks

Two data sets have been used through the current study, the first data set represents the period from 1997 to 2005 which recorded by the ENSN and contains of 800 earthquakes. The second data set represents the period from 2006 to 2014 recorded by the ENSN and the surrounding networks (Saudi National Seismic Network (SNSN), Israel Seismic Network (ISN) and International Monitoring System (IMS) stations) and contains of 775 earthquakes. The data of the IMS stations was added to the earthquakes recorded through 2009 and 2010. Figure (1) shows the recorded seismic activity of the study area for a period from 1997 to 2014. The waveforms of events recorded by the ENSN were available, while the arrival times of P and S phases were provided by the SNSN, ISN and IMS.

Historically, Egypt is considered as one of few countries that started instrumental earthquake recording in 1899. The Egyptian National Seismological network (ENSN) was established in 1997 and consisted of 76 seismic stations cover the Egyptian Territory as shown in figure (2), 49 stations

are short period, while 27 are broadband ones. Almost most of the ENSN seismic stations are established around the study area for observing its seismic activity.

Saudi National Seismological Network SNSN was established in 2005. SNSN is consists of 180 seismic stations. The SNSN includes some local networks monitoring the seismic activity that happened in the volcanic fields of the Arabian shield. All the stations operated by the SNSN have broad and very broadband seismic sensors. The eastern side of the Gulf of Aqaba and red sea have a dense stations distribution in order to record and locate the seismic activity of the Red Sea and Gulf of Aqaba. Figure (2) shows the distribution of stations for all used networks.

In the Levant region, 31 seismic stations were combined with ENSN and SNSN for locating the seismic activity of the study area. Most of these seismic stations belong to Israel Seismic Network (ISN) and two International Monitoring System (IMS) stations located in Eilat and Meron sites.

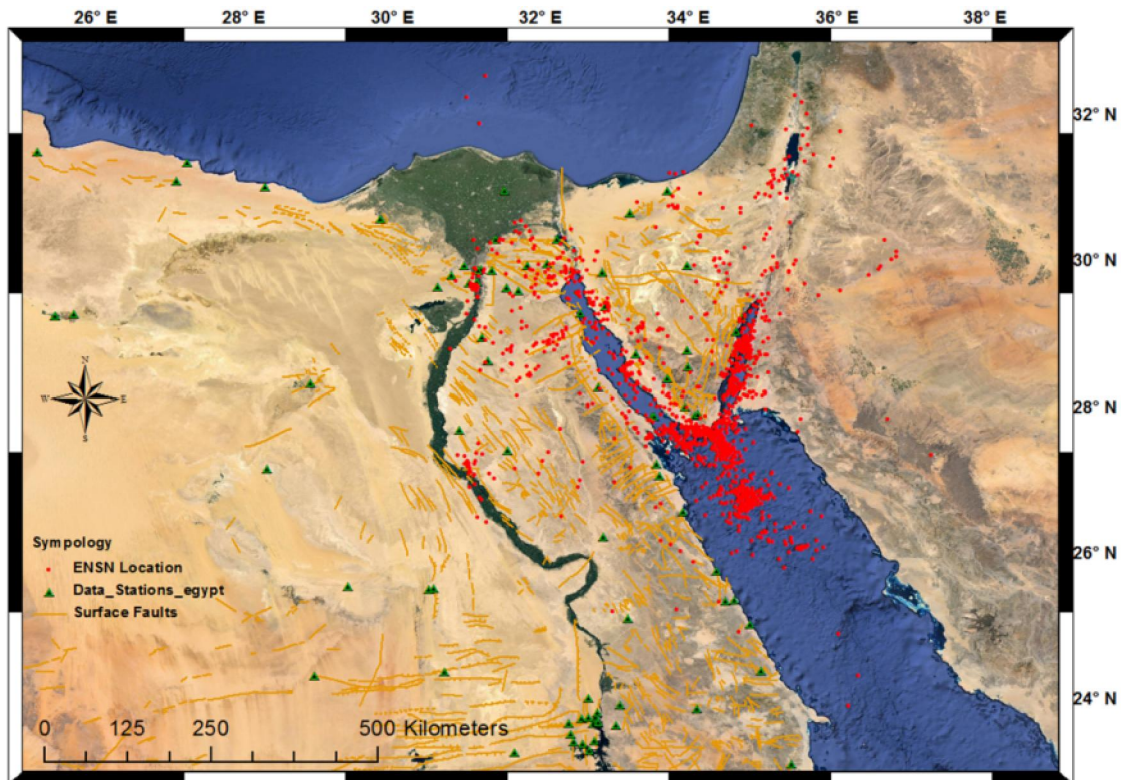


Figure (1) earthquakes located only by the Egyptian National Seismic Network (ENSN). Red dots represent the data set occurred in the study region from 1997 to 2014.

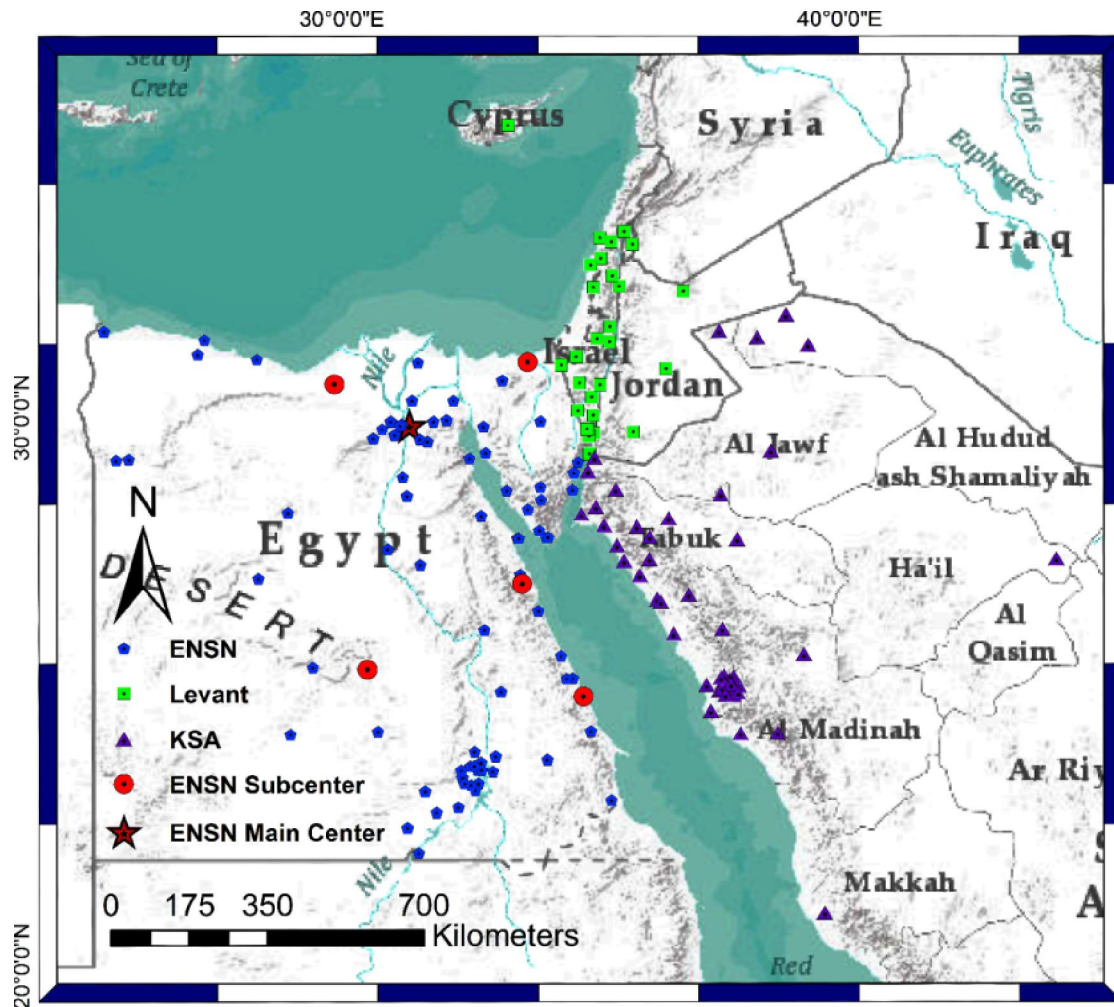


Figure (2): Distribution of seismic stations used in the current study.

Methods and data analysis

Three techniques were applied for improving the locations of the seismic activity around the study region; least square method (Lawson and Hanson, 1974), the Wadati diagram method (Wadati, 1933), and the Probability method for the determination of earthquake epicenters, Geiger (1912), and Lawson and Hanson (1974). Since the waveforms of the ENSN were available, re-picking for the seismic phases was implemented via least square method to minimize the time residuals of the picked seismic phases. For the all seismic data used (ENSN, SNSN, ISN and IMS), a physical test for the arrivals of the P and S phases was performed by using the Wadati method (Wadati, 1933) to obtain more reliable phase

picking. Using the Hypoinverse 2000 software (Klein, 2001), the final locations were obtained by applying the Probability method for the determination of earthquake epicenters Geiger (1912), and Lawson and Hanson (1974).

1) Least square method

Least square methodology (Lawson and Hanson, 1974) was implemented through Atlas software package (Nanometrics, 2005). The least-square method is an iterative procedure used to minimize the differences between the observed and theoretical travel times. Waveforms of 1814 earthquakes recorded by ENSN were used in the least square technique, an example for seismic data re-picking see figure 3.

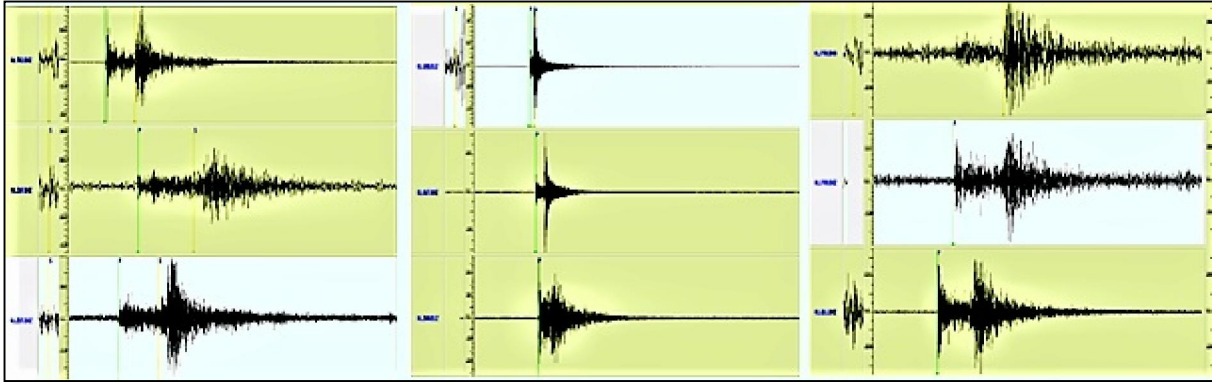


Figure (3) Examples of repicking for some events to increase number of phases for each event In order to improve reliable locations to all seismic data and chance to use the Wadati diagram.

Three velocity models of EMAM (Marzouk, 1987), HADIDY (El-hadidy, 1995) and KHRIBY (El Khreby, 2008) were used to construct the theoretical travel times for every event. The minimum average residuals were obtained using the velocity model of HADIDY (figure 4). Re-picking process increased the number of phases from 24212 to 31941 which increased the chance for applying the Wadati Diagram method as it need at least 3 couples of P and S phases for each event.

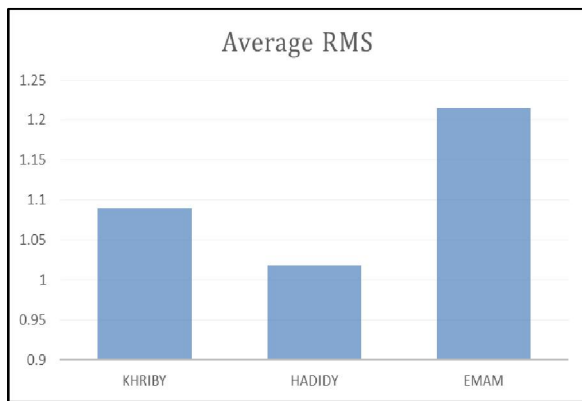


Figure (4) the Average RMS for the three models used for the dataset.

2) Wadati method

The Wadati diagram method (wadati, 1933 and Carik and Engdahl, 1973) approve a linear relation between $(T_s - T_p)$ and T_p where T_s and T_p are the arrival times of S and P phases respectively, assuming that the V_p/V_s ratio is fixed. It is used for the following:

- Obtaining the origin time of an earthquake.
- Calculating the hypocenter distances.
- Obtaining the V_p/V_s ratio (or Poisson's ratio) in a medium.

d) Examining P and S arrival times.

In the current study we used the Wadati for examining the P and S phase readings and calculating the regional V_p/V_s represents the study area, which will be used in the final earthquake locations.

A linear relation for each earthquake is computed using least square method in which;

$$V_p/V_s = 1 + (\text{slop of Wadati straight line})$$

Novotny et al, 2016 defined the deviation between the average Wadati line deduced from the earthquake and each phase (P and S phase's couple) by equation;

$$D_{wad} = (T_s - T_p)_{obs} - (T_s - T_p)_{wad}$$

Where, D_{wad} is the deviation between the Wadati straight line and the P- S phase's couple.

Since the study area is large (500 Km X 600 Km) and has complex crustal structure, Considering a fixed V_p/V_s ratio is useless and therefore a sample of 10 large well distributed earthquakes (Having high signal to noise ratio) were selected to obtain proper D_{wad} error level.

So that a test sample has been made from the largest 10 earthquakes (well distributed on the study area and has the most clear phase arrivals on its waveform) in order to find the accepted Wadati standard deviation level with best Wadati enhancing statistics and best RMS of location controlled by reliable picking. As shown Table (1) the optimum Wadati standard deviation (D_{wad}) is 2 rather than 1 due to unstable V_p/V_s ratio in the study area.

For each earthquake we achieved this via iterative approach (Stages of repicking) for maintaining the reliability and stability of the Wadati line. Therefore, repicking with guarding the reliability of all couples arrivals was implemented in order to reduce its Wadati deviation through three stages, as the following:

Stage 1: to get all earthquakes couples to Wadati deviation less than four which was done via two tries and distribution of couples in Wadati diagram shown in figure(5).

Table (1). Large 10 earthquake and its Wadati enhancing statistics; STD of Wadati(WSTD), Vp/Vs and location error with respect to variation of Accepted Wadati Error Level (AWEL)

AWEL	Q 1 WSTD	Q 2 WSTD	Q 3 WSTD	Q 4 WSTD	Q 5 WSTD	Q 6 WSTD	Q 7 WSTD	Q 8 WSTD	Q 9 WSTD	Q 10 WSTD	Average Wadati STD	Vp/Vs	Vp/Vs STD	Average Location RMS
1	2.348	1.785	0.357	0.749	0.334	1.387	0.094	0.969	1.265	0.646	0.9934	1.898	0.70867	1.221
1.5	0.988	1.834	0.357	0.641	0.732	1.032	0.094	2.069	0.382	0.658	0.8787	1.933	0.63475	1.118
2	0.988	1.896	0.357	0.871	0.732	1.08	0.094	1.017	0.382	0.962	0.8379	1.932	0.50033	1.032
3	0.988	1.896	0.357	1.814	0.732	1.366	0.094	1.017	0.976	0.712	0.9952	1.923	0.57631	1.204
4	0.988	1.896	0.357	1.814	0.732	1.643	0.094	3.813	2.145	0.712	1.4194	1.93	1.09204	1.825
Original data	0.988	4.178	0.357	1.814	0.732	1.643	0.094	2.635	2.359	2.091	1.6891	1.942	1.22219	2.145

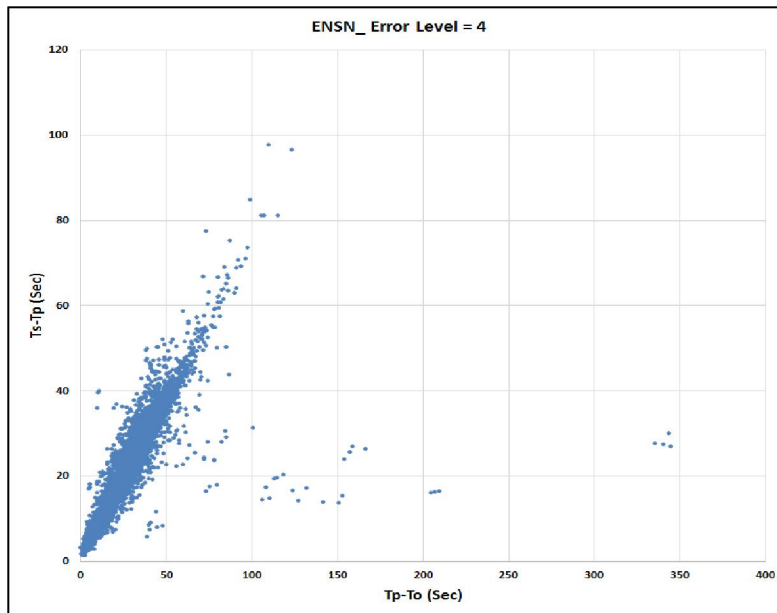


Figure (5). Distribution of earthquakes couples in Wadati diagram (stage 1).

Stage 2: to get all earthquakes couples to Wadati deviation less than three which was done via two tries and distribution of couples in Wadati diagram shown in figure(6).

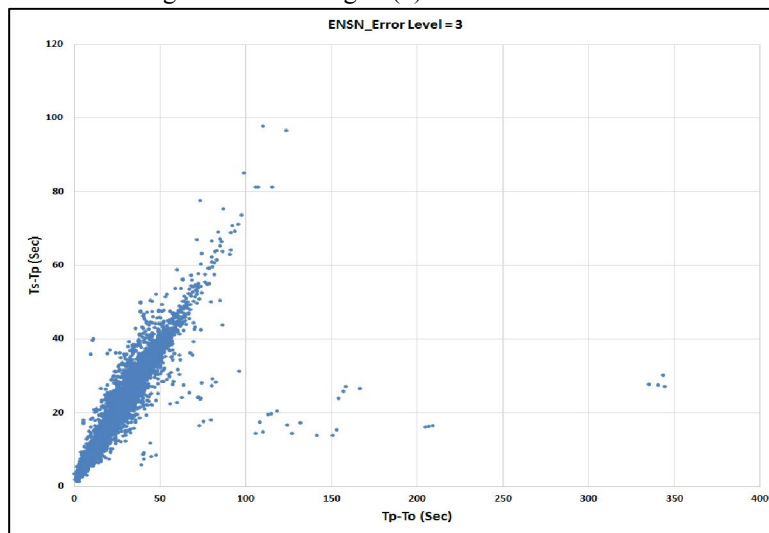


Figure (6). Distribution of earthquakes couples in Wadati diagram (stage 2).

Stage 3: to get all earthquakes couples to Wadati deviation less than two which was done via four tries and distribution of couples in Wadati diagram shown in figure(7).

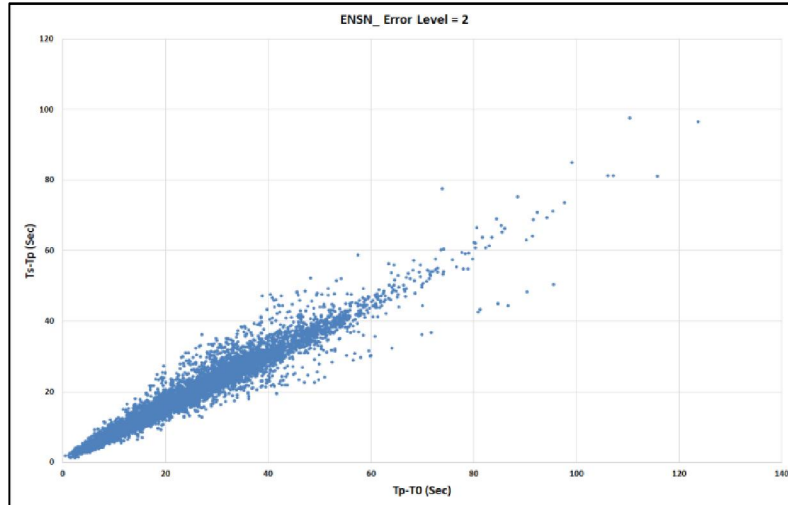


Figure (7). Distribution of earthquakes couples in Wadati diagram (stage 3).

The standard deviation for the data recorded by ENSN (1453 events; 8865 couple of P-S arrival) is $DW=0.078$, and the average estimate of $V_p/V_s = 1.768$. While after adding the arrivals from other networks (SASN & stations located in Levant region)

for 1561 events with 10337 couples, the Standard deviation was $DW=0.076$, and the average estimate of V_p/V_s is 1.767. The final distribution of couples in Wadati diagram is shown in figure (8).

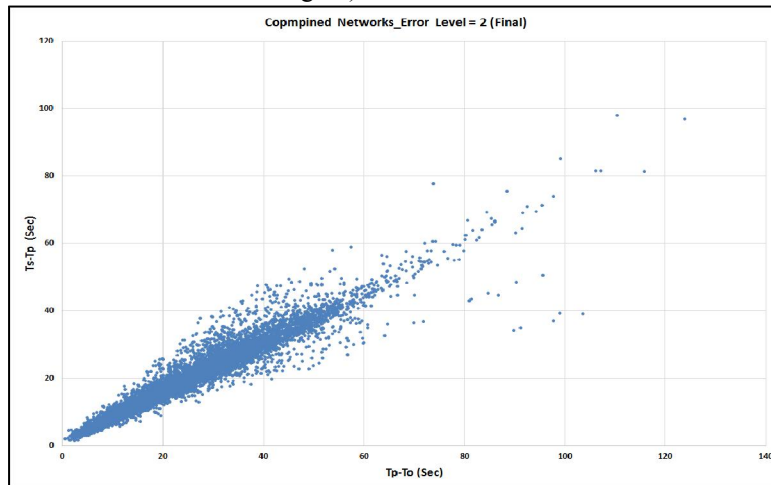


Figure (8) Final Wadati enhancing after contributing phases from regional networks

Then at the final stage, we relocated all data set by using the Hypo-inverse program with standard parameters to enhance the accuracy of location.

3) Hypo-inverse Programme

The Hypo-inverse is a Fortran Program that processes files of seismic station data for an earthquake (like p wave arrival times and seismogram amplitudes and durations) into earthquake locations and magnitudes. It was originally written for the Eclipse minicomputer (Klein, 1978). A revised version was later expanded to include multiple crustal models and other capabilities (Klein, 1989), at the

United States Geological Survey (USGS). For the locations, we used the obtained enhanced picking data set and El-Hadidy (1995) velocity model with adding the phases from the networks mentioned above (Kingdom Saudi Arabia & Levant) and guarding standard parameters in Hypoinverse solution process.

Due to lake of observations in addition to high signal to noise ratio (S/N) number of 116 events were eliminated. Therefore, the final number of earthquakes that enhanced in its locations is 1445 as

shown in Figure (9), with duration magnitudes range from 2.6 to 6.2.

Results and discussions

Three techniques have been used for improving our seismicity relocations of the study region, the Wadati diagram, the least squares method, and Hypoinverse programs. By which, increasing number of seismic phases are added to constraint the locations of the seismic activity. An improvement in locations of the ENSN bulletin have been observed after applying the previous strategies and methodology, and the reliability was increased by new picking with adding extra phases and observations, Figure(9).

After enhancement of picking for all data set guided by least square and Wadati methods, the epicentral locations were improved through stages of repicking as shown in figure (10).

When considering the comparison before and after adding other regional networks, as can be seen in figure (10), clusters of seismicity is found after using the combined networks with Wadati and least square enhancing. This cluster seismicity is inked and attached with the tectonic faults cut the study region, in parallel with the tectonic regime of

the area. Three shapes of elongated seismicity have been observed at the intersection areas of the triple junction. One is elongated towards the Levant transform fault (Gulf of Aqaba), one towards the opening of the Gulf of Suez, and the third at the Northern Red Sea part, see figure (11).

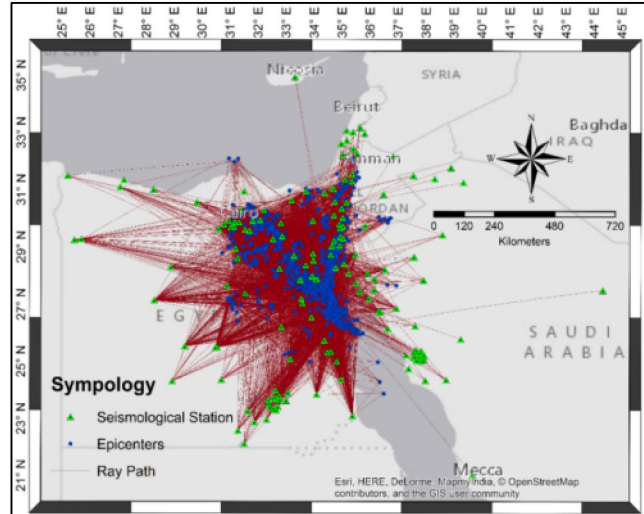


Figure (9). Seismicity relocations with adding regional stations and phases.

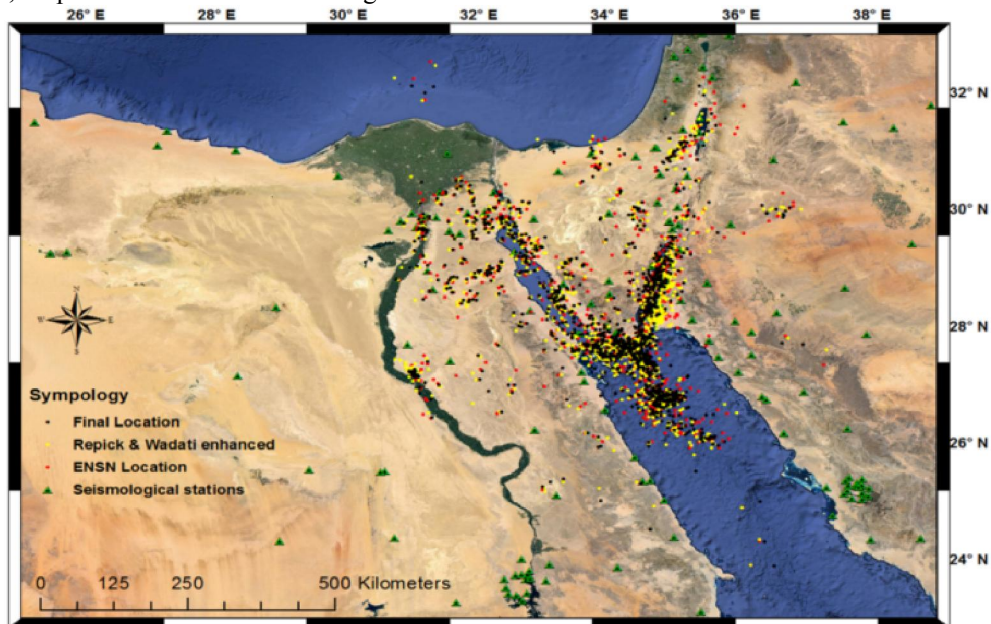


Figure (10). The enhancing in final locations for all data set. Different symbols and colors represent different stages of locations, (ENSN Catalogue, repicking with Wadati and final hypo inverse relocation).

The average horizontal dislocation in epicenters was measured at 12.790 Km, while the average Vertical dislocation in Hypocenters is 7.639 Km, Figure (10). The latitude and longitude profiling as

observed in Figure (12) shows horizontal and vertical improvement in hypocenter locations, where cluster seismicity also has been indicated.

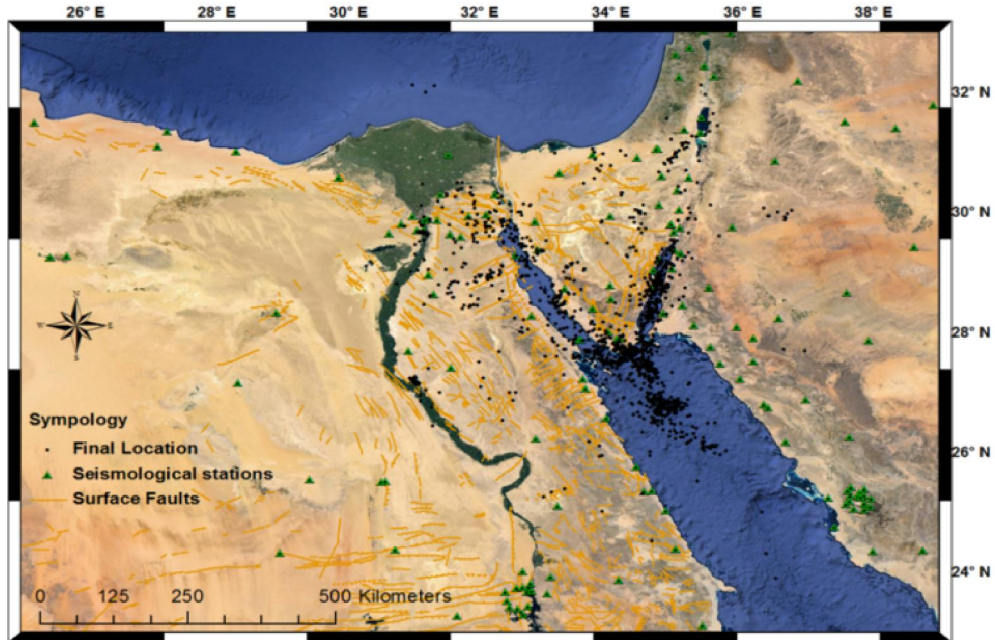


Figure (11). Final locations, clusters of seismicity around the triple junction area were observed.

In order to reveal the difference in locations before and after applying our procedures, with adding new picking of regional networks, we selected fifty events to image the shift in its locations before and

after locations using only the ENSN observations. Some events were shifted up to ~40 km to its new locations, as be seen in Figure (12).

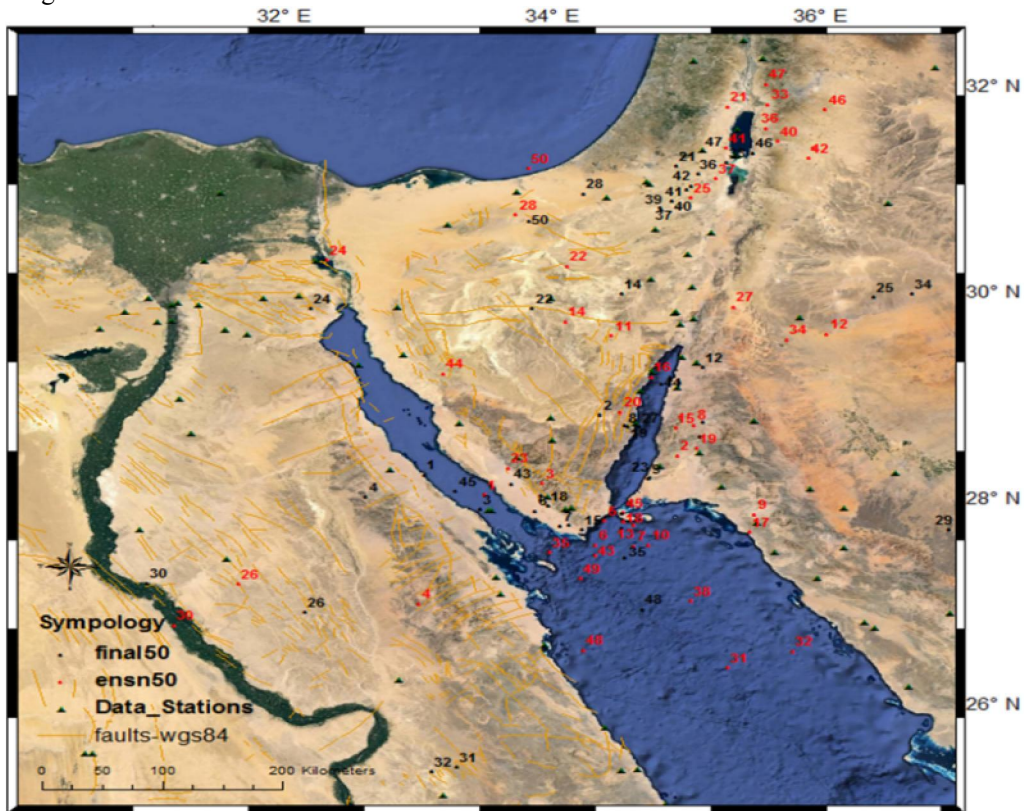


Figure (12). Relocation results for the selected fifty events, large shifts are obtained.

Through the relocations, the average errors RMS value reduced from 0.448 to 0.336 (~24.82%), the horizontal error reduced from 4.32 Km to 4.18 Km (~3.27%), and Vertical error from 13.05 Km to 11.09 Km (15.02%). Figure (13) clears the average errors among the applied relocations steps.

The average horizontal displacement in epicenters was measured at 12.790 Km and the average Vertical displacement in Hypocenters is 7.639 Km, as shown in figure (14). While the latitude and longitude profiling shows vertical improvement in hypocenter locations, Figure (15).

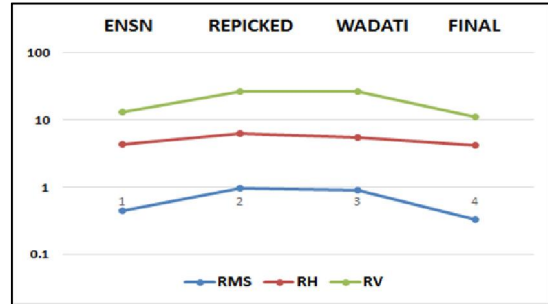


Figure (13), RMS, Horizontal and vertical Errors through relocation steps; 1) Original ENSN catalogue solution; 2) Repicked the dataset by Atlas; 3) Enhanced picking by Wadati; and 4) Final Location by Hypoinverse program.

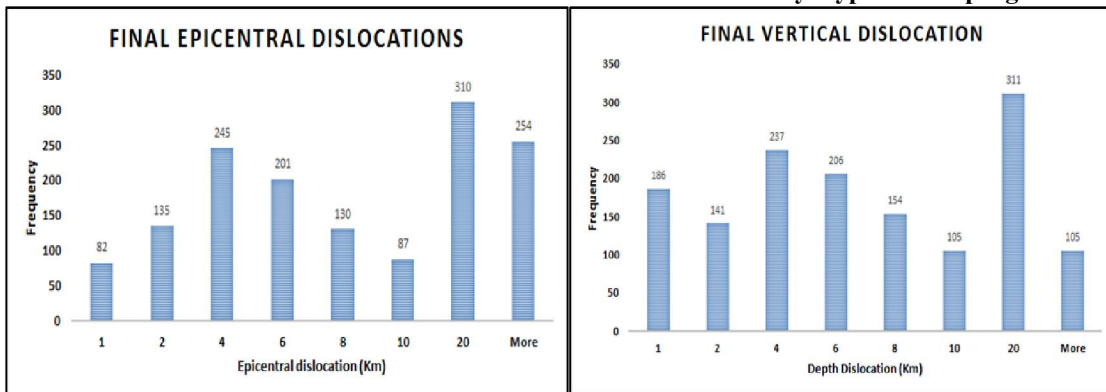


Figure (14) Final horizontal and vertical displacements histogram for the dataset

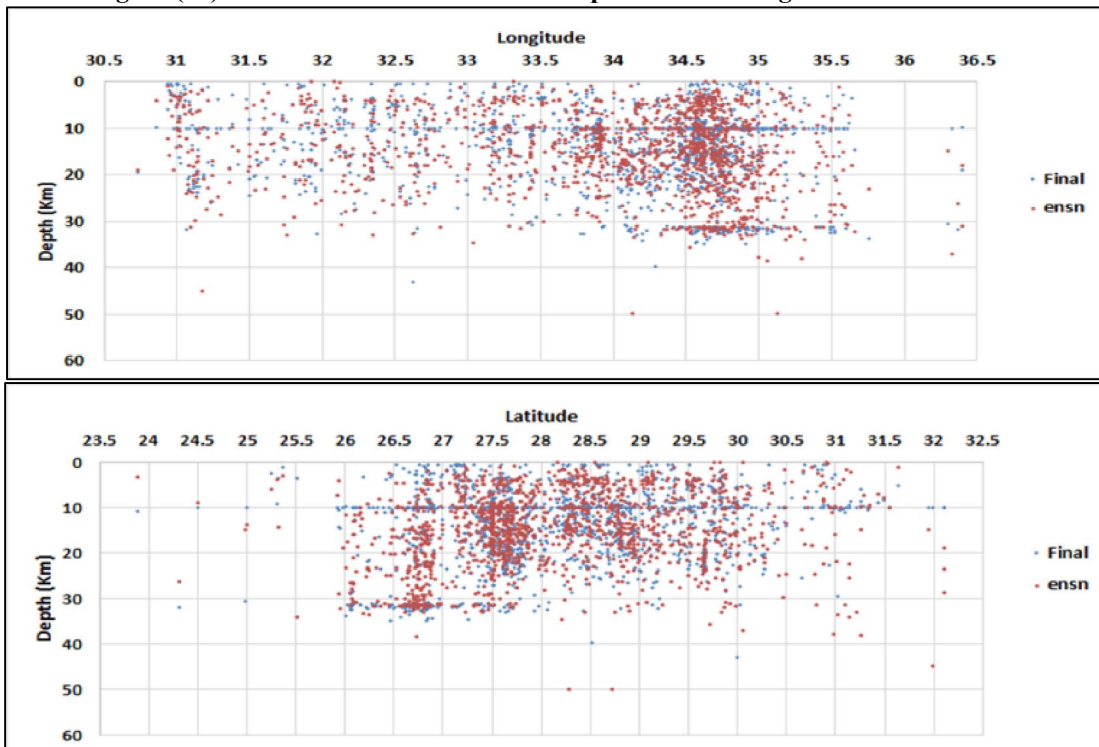


Figure (15) latitudes and longitudes profiling for the data set, shifts in longitudes are observed between locations of ENSN and adding regional networks.

Conclusions

By reducing lack of observations, increasing seismic phases from ENSN and adding arrivals from other regional seismic networks, we relocated a number of 1445 local and regional earthquakes occurred in and around the Sinai area. The Hypoinverse program was used to locate the data set for a period from 1997 to 2014 by involving 19071 phases from 176 Seismic station, Figure (9). The location reliability and the accuracy are increased with increasing seismic phase's pickings through applying the Wadati method. The output results revealed an improving in locations of local and regional earthquakes. And the seismicity was scattered with large horizontal and vertical error before applying our procedures, while became more attached around the active tectonic area, around the triple junction in after. The clustered relocated seismic activity inferred the trends of faults cut the study area. Some are clustered

around the trend of Suez Gulf (northwest-southeast), and others around the Gulf of Aqaba (northeast-southwest), while the third one linked to the intersection point among these trends (Northern Red Sea), as shown in; Figures (11, 14, 15, and 16) respectively.

Compared to previous studies, **Mamoun and Ibrahim, 1978; Mamoun et al., 1984; Atyia, 1997; and Badawy 2005** related to seismicity or seismic hazard assessment, our results provide an enhancement in locations than the previous studies since we use more phases and other arrivals from other seismic network. The output of this study is considered a new contribution for further seismic hazard studies by providing a more precise seismic catalogue of the recorded events in the study region from 1997 to 2014. Hence this provided catalogue may use for any other seismological applications.

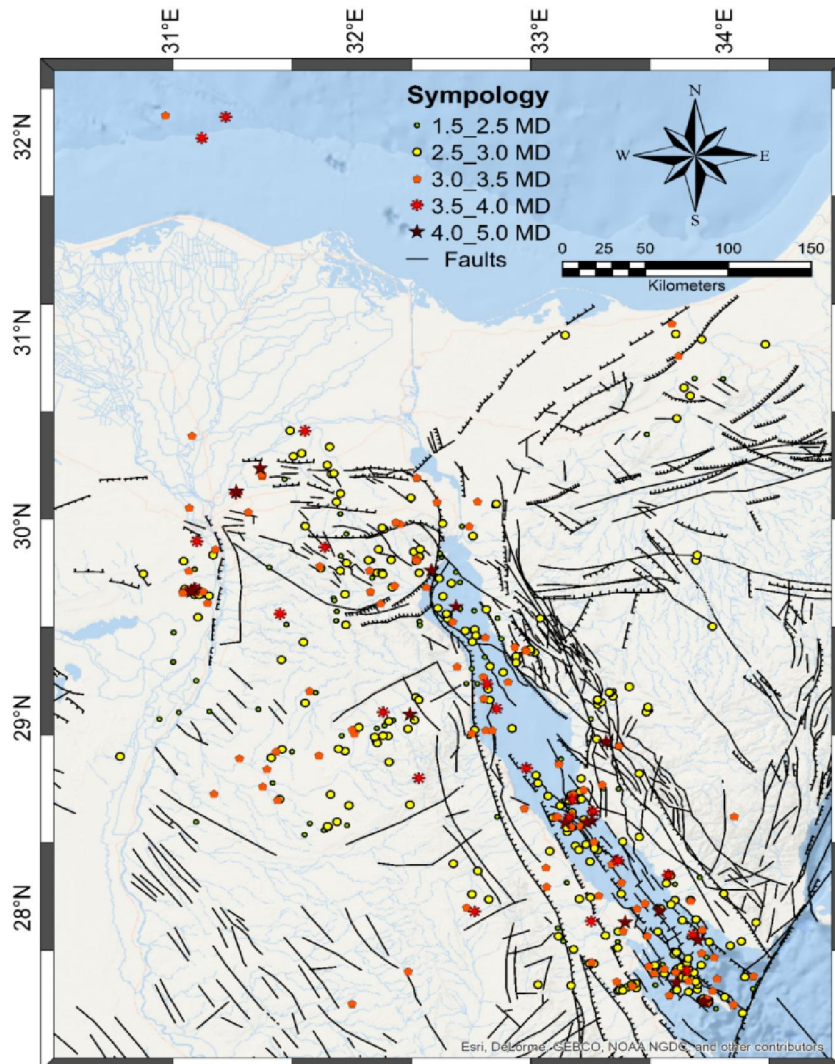


Figure (14) enhanced seismicity locations for Gulf of Suez data from 1997 to 2014.

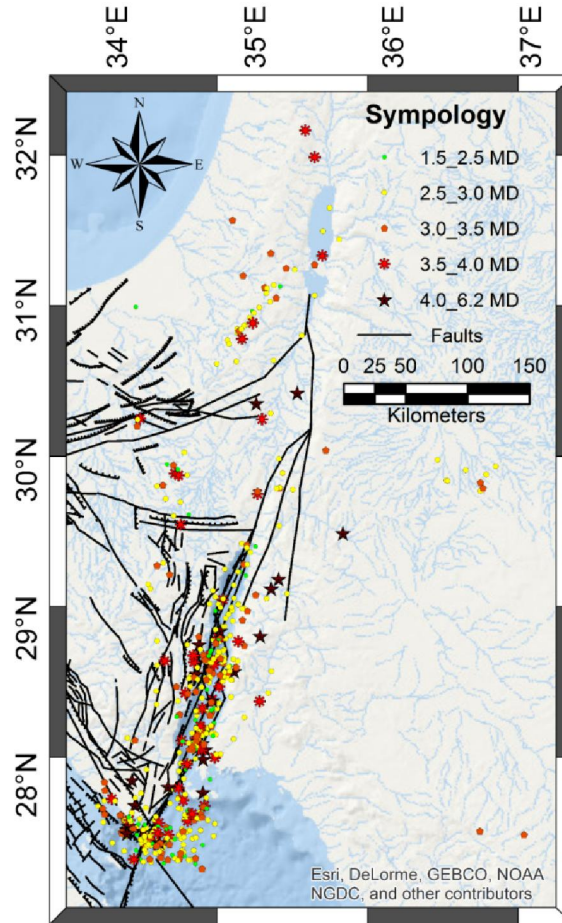


Figure (15) enhanced seismicity locations for Gulf of Aqaba data from 1997 to 2014.

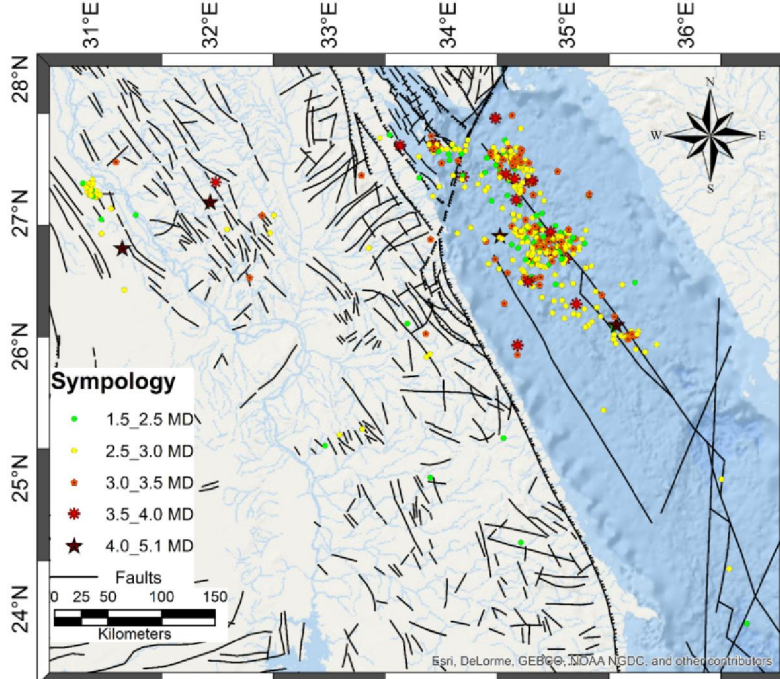


Figure (16) enhanced seismicity locations for Northern Red Seadata from 1997 to 2014.

Acknowledgement

We are grateful for the Saudi Arabia Geological survey (SASN) as well as the Egyptian National seismic network (ENSN) for providing us with seismic data needed. Also we express our deep thanks to the support from the Faculty of Mathematics and Physics, Charles University in Prague and the International Center for Theoretical Physics (ICTP), by which the current study was conducted during the regular associate visits.

References

1. Abdel-Fattah, R., (1999). Seismotectonic Studies on the Gulf of Suez Region, Egypt. M.Sc. Thesis. Fac. of Sci., Geology Dept. Mansoura Univ.
2. Abdel Rahaman, M., Tealeb, A., Mohamed, A., Deif, A., AbouElenean, K., El-Hadidy, M.S., 2008. Seismotectonic zones at Sinai and its surrounding. In: First Arab Conference on Astronomy and Geophysics, Helwan, Egypt, 20–22 October 2008.
3. Agath, A., 1981. Structural map and plate reconstruction of the Gulf of Suez Sinai area, Internal report, Conoco Oil Co., Houston, Texas, USA.
4. Atyia, K., 1997, A Study of the Seismotectonics of Egypt in Relation to the Mediterranean and Red Sea Tectonics, *Ph.D. Thesis*, Ain Shams University, Cairo, Egypt, 191 p.
5. Badawy, A., 2005. Present-day seismicity, stress field and crustal deformation of Egypt. *J. Seismol.* 9, 267–276.
6. Bauer, J., Marzouk, A.M., Steuber, T., Kuss, J., 2001. Lithostratigraphy and biostratigraphy of the Cenomanian–Santonian strata of Sinai, Egypt. *Cretac. Res.* 22, 497–526.
7. Bosworth, W., McClay, K. R., 2001. Structural and stratigraphic evolution of the Gulf of Suez rift, Egypt: a synthesis. In: Ziegler, P.A., Cavazza, W., Robertson, A.H.F., Crasquin-Soleau, S. (Eds.). In: Peri-Tethys Memoir 6: Peri-Tethyan Rift/Wrench Basins and Passive Margins, vol. 186. *Memoires du Museum National d’Histoire Naturelle de Paris*, pp. 567–606.
8. Cochran JR., 1983. A model for development of Red Sea. *Am Assoc Pet Geol Bull* 67:41-69.
9. Eaton, J. P., 1969. HYPOLA YR, a computer program for determining hypocenters of local earthquakes in an earth consisting of uniform flat layers over a half space, U. S. Geol. Surv. Open-File Rept., 155 pp.
10. El-Hadidy, S., 1995, Crustal structure and its relate causative tectonics in northern Egypt using geophysical data: Ph.D Thesis, Ain shams university, Egypt.
11. El Shazly, E.M., Abdel Hady, M.A., El Kassas, I.A., El Shazly, M.M., 1974. Geology of Sinai Peninsula from ERTS-2 Satellite Images. *Rem. Sens, Center, Cairo.* 10 pp.
12. Gardosh, M., Reches, Z., 1990. Holocene tectonic deformation along the western margins of the Dead Sea. *Tectonophysics*, 180 123-137
13. Garfunkel, Z., 1981. Internal structure of the Dead Sea leaky transform (rift) in relation to plate kinematics. *Tectonophysics*, 80: 81-108.
14. Geiger, L. 1912. Probability method for the determination of earthquake epicenters from the arrival time only. *Bull. St. Louis Univ*, 8(1), 56-71.
15. Ginat, H., Enzel, Y. and Avni, Y., (1998): Translocated Plio-Pleistocene drainage systems along the Arava fault o the Dead Sea transform. *Tectonophys.*, 284, 151-160.
16. Hosny A., Omar K., and Ali S. M., 2013. The Gulf of Suez earthquake, 30 January 2012, northeast of Egypt, *Rind. Fis. Acc. Lincei*, Vol. 24, p 337-386.
17. Hosny A. and Mervat M. Refat, and Ryan A., 2015. Crustal movement and crustal structure of the Gulf of Suez margins, *J. of Spatial Science*, Vol. 60, 387-401.
18. Hosny A. and Nyblade A., 2016. Crustal structure of Egypt and northern Red Sea region, *Tectonophysics*, 687, 257-267.
19. Carl K. and ENGD AHL R., 1973. The Interpretation of The Wadati Diagram With Relaxed Assumptions, *Bulletin of the Seismological Society of America*. Vol. 63, No. 5, pp. 1723-1736.
20. EL-Kherpy, S. A., Detailed Study of Seismic Wave Velocity and Attenuation Models using Local Earthquakes in the Northeastern Part of Egypt, Ph.D. Mansoura University, Egypt.
21. Klein, F. W. (1978). Hypocenter locations program HYPOINVERSE. US Department of the Interior, Geological Survey.
22. Klein, F. W. (1989). User's guide to HYPOINVERSE, a program for VAX computers to solve for earthquake locations and magnitudes (No. 89-314). US Geological Survey.
23. Klein F. W. 2001 User's Guide to Hypoinverse - 2000, a Fortran Program to Solve for Earthquake Locations and Magnitudes (4/2002 version 1.0); USGS Open File Report 02 - 171, p. 123.
24. Kuss, J., and Lepping, U., 1989. The early Tertiary (middle-late Paleocene) limestones from the western Gulf of Suez, Egypt.

- Neues Jahrbuch Geologie Palaontologie Abhandlungen, 177, 3, pp. 289–332.
25. Kuss, J., 1992. The Aptian–Paleocene shelf carbonates of northeast Egypt and southern Jordan: establishment and break-up of carbonate platforms along the southern Tethyan shores. *Zeitschrift der Deutschen Geologischen Gesellschaft*, 143, 107–132.
 26. Lawson, C. L and Hanson RJ 1974. *Solving Least Squares Problems*, Prentice-Hall, Inc., Englewood Cliffs, New Jersey, T.p. verso p. 312-326..
 27. Le Pichon, X., and Francheteau, J., 1978. A plate tectonic analysis of the Red Sea-Gulf of Aden Area, *Tectonophys.*, 46, 369-406.
 28. Maamoun, M. and Ibrahim, E., 1978 .Tectonic activity in Egypt as indicated by earthquake. Helwan observatory, Bull. No. 170.
 29. Maamoun, M., Allam, A., and Megahed, A., 1984. Seismicity of Egypt. *Bull. HIAG*, 109-160.
 30. Mart, X. and Hall, J., 1984. Structure trends in the northern Red Sea. *J. Geol. Res.*, 89, 352-364.
 31. Marzouk, I., 1987, Study of crustal structure of Egypt deduced from deep seismic sounding and gravity data, Ph.D. Homburg University, Germany.
 32. McKenzie, D.P., Davies, D., Molnar, P., 1970. Plate tectonics of the Red Sea and east Africa. *Nature* 226, 243-248.
 33. Moustafa, A. R., and Khalil, M. H., 1990. Structural characteristics and tectonic evolution of north Sinai folds belts, in: Said. R. (ed.), *The Geology of Egypt*.
 34. Nanometrics Inc., 2005. *ATLAS version 1.2*, Canata, Ontario, Canada.
 35. Neev, D., 1975. Tectonic evolution of the Middle East and the Levantine basin (Structural lineation map of Sinai Peninsula).
 36. Novotný, O., Málek, J. and Boušková, A., 2016. Wadati method as a simple tool to study seismically active fault zones: a case study from the West-Bohemia/Vogtland region, central Europe. *Stud GeophysGeod* (2016),60, 248.
 37. Robson, D. A., 1971: The structure of the Gulf of Suez (Clysmic) rift with special reference to the eastern side. *Journal of the Geological Society, London*, 127: 247-277.
 38. Said, R., 1962. *Geology of Egypt*. Elsevier, Amsterdam/New York.
 39. Salamon, A., Hofstetter, A., Garfunkel, Z., Ron, H., 1996. Seismicity of the Eastern Mediterranean region: perspective from the Sinai subplate. *Tectonophysics* 263, 293–305.
 40. Shata, A., 1956: Structural development of the Sinai Peninsula, Egypt. *Desert Institute of Egypt, Bulletin*, vol. 6, p. 22.
 41. Steckler, M. S., 1985. Uplift and extension at the Gulf of Suez: indications of induced mantle convection. *Nature*. 317, 135-139.
 42. Steinitz, G., Bartov, Y., Hunziker, J.C., 1978. K/Ar age determinations of some Miocene–Pliocene basalts in Israel: their significance to the tectonics of the rift valley. *Geol. Mag.* 115, 329–340.
 43. Wadati, K. 1933. On the travel time of earthquake waves. Part II, *Geophys. Mag.* 7, 101-111.
 44. Woodside, J., 1977. Tectonic elements and crust of the Eastern Mediterranean Sea. *Mar. Geophys.* 3, 317–354.

3/21/2017